Published in final edited form as:
Cancer Res. 2015 January 1; 75(1): 51–61. doi:10.1158/0008-5472.CAN-14-0820.

Paradoxical decrease in the capture and lymph node delivery of cancer vaccine antigen induced by TLR4 agonists as visualized by dual-mode imaging

Deepak K. Kadayakkara[1,2,3], **Michael J. Korrer**[1,2,3,4], **Jeff W.M. Bulte**[1,2,3,4,5,6], and **Hyam I. Levitsky**[1,2,*]

[1]Department of Oncology, The Johns Hopkins School of Medicine, Baltimore, MD

[2]Sidney Kimmel Comprehensive Cancer Center, Johns Hopkins University School of Medicine, Baltimore, MD

[3]Russell H. Morgan Department of Radiology and Radiological Science, Division of MR Research, The Johns Hopkins School of Medicine, Baltimore, MD

[4]Cellular Imaging Section and Vascular Biology Program, Institute for Cell Engineering, The Johns Hopkins School of Medicine, Baltimore, MD

[5]Department of Biomedical Engineering, The Johns Hopkins School of Medicine, Baltimore, MD

[6]Department of Chemical & Biomolecular Engineering, The Johns Hopkins School of Medicine, Baltimore, MD

Abstract

Traditionally, cell-mediated immune responses to vaccination in animal models are evaluated by invasive techniques such as biopsy and organ extraction. We show here that by combining two non-invasive imaging technologies, magnetic resonance imaging (MRI) and bioluminescence imaging (BLI), we can visualize both the afferent and efferent arms of cellular events following vaccination longitudinally. To this end, we evaluated the immune response elicited by a novel toll-like receptor 4 agonist vaccine adjuvant, glucopyranosyl lipid A (GLA), using a whole cell tumor vaccine. Following magnetovaccination, MRI was used to visualize antigen presenting cell-mediated antigen capture and subsequent migration to draining lymph nodes (DLN). Paradoxically, we observed that the incorporation of GLA in the vaccine reduced these critical parameters of the afferent immune response. For the efferent arm, the magnitude of the ensuing antigen-specific T cell response in DLN visualized using BLI correlated with antigen delivery to the DLN as measured by MRI. These findings were confirmed using flow cytometry. In spite of the GLA associated reduction in antigen delivery to the DLN however, the use of GLA as a vaccine adjuvant led to a massive proliferation of vaccine primed antigen-specific T cells in the spleen. This was accompanied by an enhanced tumor therapeutic effect of the vaccine. These findings suggest that GLA adjuvant changes the temporal and anatomical features of both the

*Corresponding Author: Dr. Hyam I. Levitsky, M.D., Department of Oncology, 1650 Orleans Street, Rm. 472, Sidney Kimmel Comprehensive Cancer Center, Johns Hopkins School of Medicine, Baltimore, MD 21287; hy@jhmi.edu, 410-614-3616.

Conflict of Interests: The authors have no conflict of interests to disclose

afferent and efferent arms of the vaccine response and illustrates the utility of quantitative non-invasive imaging as a tool for evaluating these parameters during vaccine optimization.

Keywords

TLR4 agonist; vaccine adjuvant; magnetovaccination; cell tracking; cancer immunity

Introduction

Comprehensive visualization of distinct stages of the immune response to vaccination *in vivo*, ranging from the capture of antigen and migration of APCs to ensuing T cell priming, is a potentially powerful tool for the evaluation of vaccination strategies and the design of novel vaccine formulations. Invasive techniques such as biopsy of the vaccination sites, extraction of lymphoid tissues, and sampling of circulating lymphocytes and antibodies are the current gold standards in assessing the impact of novel vaccine strategies on cell mediated immune responses. Drawbacks of these methods are the inability to monitor the response to vaccination in the same subject longitudinally and the inability to evaluate the immune response occurring in a subject as a whole, thus introducing sampling bias. Non-invasive imaging methods such as magnetic resonance imaging (MRI) and bioluminescence imaging (BLI) can significantly improve our understanding of vaccine-mediated immune response because they provide a unique opportunity to visualize the immune cell dynamics longitudinally in whole organisms from beginning to end(1).

In this report, we investigated the use of dual-mode imaging (MRI and BLI) for evaluating the efficacy of a tumor cell-based vaccine platform (GVAX) in which irradiated tumor cells are engineered to secrete granulocyte monocyte colony stimulating factor (GM-CSF). GVAX has been shown to induce strong cell mediated anti-tumor immune responses in a variety of preclinical models and in humans (2, 3). The paracrine production of GM-CSF leads to the recruitment of immune cells to subcutaneous or intradermal vaccination sites and the differentiation of precursor cells to APCs resulting in the uptake of tumor antigens released by the irradiated cells in the vaccine. Captured antigen is then transported by APCs via afferent lymphatics to DLN where T cell priming ensues (4). However GM-CSF does not directly activate APCs to full maturation, which is thought to be required for their optimal trafficking to DLN and acquisition of full T cell stimulatory capacity. Toll like receptors (TLR) are specialized receptors that activate APC such as macrophages and dendritic cells (DC) and enable them to process and present antigens efficiently to T cells (5-7). Recent studies have shown that TLR agonists are efficient vaccine adjuvants against infectious diseases and cancer (7). Vaccine adjuvanticity depends on the ability to mature APCs at the site of vaccination, induce APCs to migrate via lymphatics to DLN, process the antigens efficiently, increase the expression of co-stimulatory molecules and cytokines, and present the antigens to T cells in the appropriate lymphoid microenvironment to stimulate effector immune response. TLR4 is expressed on the surface of APCs (5) and upon by binding to ligands, such as bacterial lipopolysaccharide (LPS) or HSP 60 and 70, activate APCs through the MyD88 pathway (8). Although LPS is a very effective activator of APCs, it can have significant toxicity that has precluded it from being used as vaccine adjuvants.

The toxicity problem has been circumvented by developing synthetic molecules that are more selective for TLR4, with no effect on vascular permeability (9). Glucopyranosyl Lipid A (GLA) is a synthetic glycolipid that stimulates APCs via TLR4, induce a type 1 immune response, and increase immunogenicity to vaccine antigens (10, 11). The unique immunomodulatory properties of GLA make it an attractive adjuvant that can be combined with GVAX. The rationale for such a combination is that each will act sequentially and synergistically to improve tumor immunity. The GM-CSF component of the vaccine recruits and differentiates precursor cells to APC and the GLA component activates APC and creates an inflammatory milieu driving a Th1 immune response. GLA used as adjuvant with GVAX as an intra-tumoral vaccine has been shown to increase the recruitment of immune cells to the tumor microenvironment, inducing cytotoxic T cells and leading to better tumor therapeutic effects compared to GVAX alone (12). However, the effect of GLA as a vaccine adjuvant when the vaccine is administered in distant sites from the tumor has not been investigated before.

The magnitude of the T cell response to vaccination is thought to be in part dependent on the magnitude of antigen delivery to DLN by appropriately matured APCs (13). The effects of TLR4 agonists on the extent of antigen capture and delivery by APCs and the ensuing T cell response has not been systematically evaluated before. It is critical to understand the influence of TLR4 and other adjuvants being developed on these discrete steps of the immune response to optimize vaccine efficacy.

Magnetovaccination is a recently described cellular MRI based technique devised to visualize APC mediated transport of antigen to the DLN (14). In this method, whole cell tumor vaccine is labeled with superparamagnetic iron oxide (SPIO) nanoparticles. Following *in vivo* transfer of antigen/nanoparticles from the vaccine to APCs, their migration to the DLN can be visualized and quantified using MRI. This technology has a spatial resolution of 75 μm^3 and is capable of visualizing DLNs in mice of few millimeters with exceptional clarity. It is also well suited for clinical translation as it can in principle be directly applied to human subjects without further modifications. SPIO nanoparticles have been used to track *ex vivo* labeled DCs in humans (15). BLI using luciferase reporter genes has been used to study cell migration and proliferation of immune cells, stem cells and cancer cells (16). It is a robust imaging technique which has been widely used in rodents.

In this study, MRI and BLI were used to systematically visualize the afferent and efferent arms of cellular response to vaccination, respectively. Using a GVAX vaccine formulated against poorly immunogenic B16-melanoma, we examined the effects of the TLR4 agonist GLA as a vaccine adjuvant with GVAX. Our results show that addition of GLA to GVAX not only significantly alters APC-mediated antigen capture and delivery but also the nature and sites of T cell priming and expansion. We believe that our dual-mode imaging approach can serve as a platform technique to screen and evaluate a variety of experimental vaccine-adjuvant systems.

Materials and Methods

Cell Culture

B16-mOva cells were cultured in complete RPMI medium supplemented with 10% FBS, 1% penicillin/streptomycin and 0.1% 2-mercaptoethanol under G418 (1.0 mg/ml) selection. B78H1GM cells were cultured in the media described above with the addition of hygromycin (1.2 mg/ml) selection.

Cell labeling with nanoparticles

B16-mOva cells were grown at about 80% confluence in their logarithmic stage of growth. The media was removed and cells were incubated in fresh media containing wFION(17) at a concentration of 50 μg/ml or Molday Ion EverGreen (Biopal, Cambridge, MA) at a concentration of 50 μg/ml for 24 hours at 37°C. Cells were washed three times after labeling, trypisinized, and harvested. Cell viability was assessed by trypan blue staining.

Prussian blue staining

Labeled cells were fixed with 2% paraformaldehyde for 15 minutes and washed three times with PBS. Prussian blue staining was performed using a Prussian blue kit (Biopal, Cambridge, MA). Cells were incubated in the staining solution for 20 minutes and washed three times with PBS. Cells were imaged using an inverted microscope (Olympus IX73, Center Valley, PA).

Vaccination

B16 or B16-mOva cells and B78H1GM cells were harvested and irradiated at 10,000 rads using a Gammacell 1000 irradiator. 1×10^6 B16 cells were mixed with 1×10^5 B78H1GM cells to produce the GVAX vaccine. B78H1GM cells secrete GM-CSF at 3 μg/1×10^6 cells/24 hours(18). Cells were resuspended in 20 μl of PBS. GLA was purchased from Immune Design Corporation (Seattle, WA) as stable oil in water emulsion. For vaccination with GLA, 20 μl (20 μg) was added to GVAX. In the GVAX only vaccine, 20 μl of vehicle control was mixed with GVAX. Vaccines were injected in the hind footpad.

Mice

C57/B6 regular mice and C57/B6 albino mice (female, 8-10 weeks old) were purchased from the National Cancer Institute. All animal experiments were approved by the animal care and use committee of our institute. For BLI and MRI experiments, C57/B6 albino mice were used and C57/B6 regular mice were used for tumor challenge experiments and FACS experiments. For T cell tracking experiments, a colony of OT1-Luc mice was established in our facility by crossing transgenic OT1 $Rag^{-/-}$ mice with transgenic C57/B6-$Luc^{+/+}$ mice.

Adoptive transfer of CD8+ T cells

Spleens were harvested from transgenic OT1-Luc mice and a single cell suspension was prepared by mashing the spleens over a 50 μm nylon cell strainer. Red blood cells were lysed by incubaton in 5 ml of ACK lysis buffer (Invitrogen, Carlsbad, CA) for 5 minutes at room temperature. CD8+ T cells were purified using a MACS CD8α+ negative selection kit

(MiltenyiBiotec, Cologne, Germany) following the manufacturer's protocol. Purified cells were counted and resuspended in PBS. For adoptive transfer, 4-5×10^6 purified cells in 200 μl of PBS were injected intravenously through the tail vein 24 hours before vaccination.

MRI

Mice were imaged using a Bruker 11.7T horizontal bore microimaging system (Bruker, Billerica, MA) equipped with a birdcage volume resonator. Mice were anesthetized using 2.5% isoflurane in air and under monitoring of respiration and temperature. The knee was placed in the center of the coil and axial sections were obtained through the popliteal DLNs. Images were obtained using a T2*-weighted multi-gradient-echo (MGE) sequence (TR/TE=500/4 ms, number of echoes=5, Slice thickness=0.5 mm, number of slices=15, averages=4, matrix size=256×256, FOV=22×22 mm).

BLI

Mice were imaged using an IVIS Spectrum imaging system (Perkin Elmer, Waltham, MA). The dorsal and ventral surface encompassing the abdomen and lower back of the mice were shaved before imaging. For each imaging session, 30 mg/kg body weight of D-Luciferin in PBS was injected i.p. Mice were anesthetized using 2.5% isoflurane in air and were imaged 10 minutes after the injection using the following instrumental settings: Exposure time= 5 min, F stop=1, Binning=Medium, Stage height=D.

Flow Cytometry

Cells were resuspended in flow cytometry buffer containing HBSS supplemented with 0.5% BSA and stained with the following antibodies: anti CD11c+, anti-MHC-II, anti-CD40, CD45.2, CD45.1 and anti-CD86. All antibodies were purchased from BD Biosciences (San Jose, CA) and conjugated to R-PE, PercP, Pacific Blue or APC. Cells were analyzed using a FACS caliber and an LSR II instrument (Becton-Dickinson Biosciences, San Jose, CA).

Quantification of MRI and BLI

Quantification of MRI was done as described previously (14). Briefly, an ROI was drawn around the DLN and a pixel intensity histogram was plotted using NIH Image J. Similarly, another ROI was drawn in the adjacent muscle tissue as a reference and the pixel intensity histogram was plotted. The lowest pixel intensity histogram in the reference ROI was determined as threshold. All pixels with intensity below this threshold were considered pixels containing APCs that captured iron oxide nanoparticles. The procedure was repeated for all the slices and added together to determine the total black pixel count in a DLN. For BLI, the images were processed using Living Image software version 4.4 (Perkin Elmer, Waltham, MA). An ROI was drawn around the DLN, spleen, footpad or the entire mice and the intensity over the integrated area over the ROI was calculated by the software and luminescence count was normalized to radiance.

Tumor model

Mice were injected s.c. with 1×10^5 B16 mOva cells resuspended in 100 μl of PBS. On day 4, mice were vaccinated with either GVAX or GVAX with GLA. For timed administration

of GLA, GLA was administered in the same footpad as the vaccine on day 3 or day 5. Tumor cross sections were measured serially using a caliper.

TIL isolation

Tumors were excised on day 18 following inoculation and digested with 5 U/mL Collagenase I (Sigma-Aldrich, St. Louis, MO), 50 U/mL DNase I (Sigma-Aldrich, St. Louis, MO), and 5 U/mL Hyaluronidase, II (Sigma-Aldrich, St. Louis, MO), for 2 hours in 10% complete-RPMI following mechanical disruption. Cells were then passed through a 40 μm filter

Results

Magnetovaccination with GLA reduces APC-mediated antigen capture and delivery to DLN

The GVAX vaccine consisted of lethally irradiated B16 melanoma cells stably transfected to express the model antigen chicken ovalbumin (B16-mOva) mixed with GM-CSF secreting B78H1GM “bystander” cells(18). GLA was mixed with GVAX thirty minutes before vaccination. The vaccine labeled with SPIO nanoparticles was administered in the hind footpad and the draining popliteal DLNs were imaged using MRI. We hypothesized that addition of GLA promotes APC maturation, leading to an increase in antigen delivery to DLN. Paradoxically however, the addition of GLA in the vaccine significantly *reduced* the number of APCs that did capture iron oxide nanoparticles in the DLN as revealed by the number of black pixels in the DLN (Fig. 1A) compared to GVAX alone. Black pixels were located in the central part of the DLN corresponding to the medulla of the DLN, where APCs meet cognate T cells. As the concentration of iron oxide nanoparticles increases within the DLN, as observed with GVAX on day 6, the blooming susceptibility effect of accumulated iron oxide nanoparticles spread to the entire DLN. The magnitude of APC migration was quantified by counting the black pixels below a threshold in a region of interest(ROI) encompassing the DLN(14). The threshold was set using a pixel intensity histogram of the adjacent muscle tissue. In both vaccinated groups, the magnitude of antigen capture was increased from day 3 to day 6. The quantitative analysis showed that GLA co-administration led to a significant decrease in the accumulation of APC captured antigen/iron oxide in DLN ($p<0.001$, two-tailed T Test).

To confirm these findings invasively, GVAX and GVAX+GLA were subsequently labeled with iron oxide nanoparticles conjugated with the fluorophore EverGreen and the DLN were extracted and analyzed on day 6 following vaccination. As predicted based on TLR4 mediated APC maturation, flow cytometry analysis revealed that total number CD11c+ cells actually increased in the DLN (Fig. 2C, $p<0.05$) with the addition of GLA. Furthermore, the total cellularity of the DLN was increased in the presence of GLA (Fig. 2D, $p<0.001$). However, consistent with the MR data, the number of APCs that did capture antigen in the DLN was significantly decreased, both as a percentage of total LN cells ($p<0.001$, two-tailed-T test) and absolute number ($p<0.0001$, two-tailed T test) of CD11c+ EverGreen+ cells (Figs. 2A and B).

Antigen capture by APC is associated with their activation profile

Upregulation of co-stimulatory molecules such as CD40 and CD86 along with MHC-II are critical determinants of the ability of APCs to present antigen to their cognate T cells and activate them. We examined the activation status of CD11c+ cells in the DLN of mice vaccinated with GVAX and GVAX+GLA. The co-stimulatory molecules CD40 and CD86 were markedly upregulated in CD11c+ cells that captured iron oxide nanoparticles conjugated to EverGreen in both the vaccinated groups (Fig. 3A). A proportion of CD11c+ cells that were not EverGreen+ also upregulated these activation markers, although not at the level of CD11c+ EverGreen+ cells. CD11c-cells did not upregulate these markers. MHC-II expression waqupregulated in CD11c+ cells irrespective of their antigen capture status in both vaccine groups. Surprisingly, GVAX formulated with GLA led to no significant change in the activation profiles of APC as compared to GVAX alone.

Antigen-specific CD8+ T cell accumulation in the DLN correlates with the amount of antigen delivered to the DLN

Priming and activation of antigen-specific CD8+ T cells is critical for effective vaccine-mediated tumor protection. The CD8+ T cell response was evaluated using BLI in the same cohort of mice that underwent magnetovaccination and MRI. We adoptively transferred ovalbumin-specific CD8+ T cells from OT1 transgenic mice that stably express firefly luciferase a day before magnetovaccination. Vaccination was done with B16-mOva GVAX, and the CD8+ T cell response was serially monitored by BLI. We observed a significantly greater accumulation of CD8+ T cells in the DLN of mice vaccinated with GVAX compared to GVAX+GLA (Figs. 4A and B). This observation correlated with the extent of APC-mediated antigen capture and delivery to the DLN. Interestingly, in mice vaccinated with GVAX+GLA, there was significant accumulation of CD8+ T cells in the spleen (Fig. 4C, $p<0.01$, two-tailed T test) and in the vaccination site (footpad) (Fig. 4D, $p<0.05$, two-tailed T test), consistent with a systemic pattern of T cell priming and expansion. Moreover, the total OT1 CD8+ T cell signal measured in each whole mouse was comparable between both groups at 7 days after vaccination (Fig. 4E), suggesting that the extent of vaccine primed CD8+ T cell expansion measured systemically was not proportional to the magnitude of the response initially occurring within the DLN.

GLA administration 24 hours after vaccination partially rescues APC-mediated antigen delivery to the DLN

Based on our observation that GLA reduces the magnitude of APC-mediated antigen delivery to the DLN, we hypothesized that administration of GLA together with GVAX may induce premature maturation of APC and prevent efficient antigen capture. In order to address this hypothesis, we timed GLA delivery 24 hours before, together with, and 24 hours after vaccination with respect to GVAX and evaluated the APC-mediated antigen delivery to the DLN by MRI and flow cytometry. Antigen delivery was reduced when GLA was administered 24 hrs before or together with GVAX. However, there was a significant increase in APC-mediated antigen delivery to the DLN when GLA was administered 24hrs after vaccination as measured at 3days after vaccination (Figs. 5A,B, $p<0.01$, two-tailed T test). In all groups, APC-mediated antigen delivery to DLN increased from day 3 to day 6

(Fig. 5B). These results were validated by flow cytometry analysis of the excised DLN (Fig. 5C,D, $p<0.01$, two-tailed T test). These results are consistent with our hypothesis that GLA prematurely induces the maturation of APCs before they can capture antigen from the site of vaccination.

Antigen-specific CD8+ T cell accumulation in the DLN correlates with antigen delivery to the DLN after timed administration of GLA

We investigated how the timing of GLA administration with vaccination influences antigen-specific T cell expansion. As in the previous experiments, OT1 T cells stably expressing luciferase were adoptively transferred a day before vaccination. GLA was administered 24 hrs before, together with, or 24 hrs after vaccination in the same footpad and serially imaged using BLI. As expected, there was increased accumulation of T cells in DLN of mice vaccinated with GVAX and GLA 24 hrs after (Figs 6A,B). However, this effect was dwarfed by the systemic nature of the activation of CD8+ T cells in all the mice vaccinated with GLA, regardless of their timing with respect to vaccination (Figs. 6 C-E).

GLA administered together with GVAX improves the treatment of established tumors

As an integrated measure of the impact of GLA on the downstream effector function of the host response to vaccination, mice were challenged with live B16-mOva cells subcutaneously in the flank and vaccinated in the footpad 4 days later, and the tumor growth was monitored serially over time. A significant delay in tumor growth was observed when GLA was administered in combination with GVAX compared to GVAX alone or when GLA was administered separately from GVAX (Fig. 7 A, $p<0.05$, two-tailed T test). Contrary to the anticipated outcome, these results suggest that in the system studied, tumor therapeutic effects do not directly correlate with the magnitude of antigen delivery to the DLN and suggest that other features of the adjuvant effect contribute to enhanced tumor rejection. To further understand the mechanism of tumor rejection, we compared the systemic trafficking and tumor infiltration of adoptively transferred OT1 cells with a congenic marker CD45.1 following vaccination. Three groups from the above tumor rejection studies were used based on the differences in the magnitude of antigen delivery to the DLN. Mice vaccinated with GVAX alone that had most antigen delivery to the DLN were compared to mice vaccinated with GVAX+GLA that had the least antigen delivery to the DLN in addition to the unvaccinated group. Mice were administered OT-1 CD45.1+ CD8 T cells 24 hours before implantation with B16-mOVA tumors. Four days following tumor injection, the mice were vaccinated with PBS, GVAX or GVAX + GLA. Tumors and spleens were isolated 18 days following tumor implantation and analyzed using flow cytometry. Analysis of tumor infiltrating lymphocytes (TIL) showed a significant vaccine-mediated trafficking of endogenous $CD8^+$ T cells and adoptively transferred CD45.1 OT1 cells into the tumor tissues in both vaccinated groups compared to the unvaccinated group (Figs. 7B,C). There is a clear trend that mice vaccinated with GVAX+GLA exhibit more OT1 infiltration in the tumors (55% of the total $CD8^+$ TILs) compared to mice vaccinated with GVAX (44% of the $CD8^+$ TILs) or unvaccinated mice (6% of the $CD8^+$ TILs). Although the trend we observed did not reach statistical significance, it was sufficient to induce significant tumor therapeutic effects (Fig. 7A). A similar trend was observed in the spleen (Fig. 7D) suggesting robust systemic expansion of T cells following vaccination.

These experiments have to be interpreted in the context that GVAX+GLA significantly reduces APC-mediated antigen transfer to the DLN while still inducing increased vaccine-mediated tumor T cell infiltration, suggesting that the T cells primed via GVAX+GLA have a more efficient systemic expansion and tumor infiltration.

Discussion

We have showed here that a combination of two non-invasive imaging techniques can be used effectively to visualize a vaccine-mediated immune response, which is potentially valuable for screening new vaccine-adjuvant systems. In contrast to traditional invasive methods, it provides an unbiased way to visualize the immune response in a whole organism. To the best of our knowledge, this is the first time where MRI and BLI are used together to comprehensively visualize both the afferent and efferent immune response induced by vaccination. This unconventional approach has led us to the discovery of previously unknown effects of GLA.

Analysis of afferent arm of vaccination led to the paradoxical observation that GLA reduced APC-mediated antigen delivery to the DLN. Although a reduced ability of phagocytosis was observed in DCs co-cultured with LPS *in vitro* (19), this effect has not been reported *in vivo*. By timing the GLA delivery with respect to GVAX, we showed that GLA induced premature maturation of APCs in the vaccination site and thus may have reduced their capacity for vaccine antigen capture prior to migration. Premature maturation of APCs and consequent reduction in phagocytosis was partially rescued by timing GLA 24 hours post vaccination. An alternate possibility is that GLA reduces the flow in afferent lymphatics. Previous immunization studies using oxazolone have shown that in first few days after vaccination, there is severe insufficiency in the afferent lymphatic vessels that can reduce the migration of DCs to the DLN. The function of afferent lymphatics is compromised in the presence of inflammation and it is likely due to increased interstitial fluid accumulation and acute inflammation causing disruption in the lymphatic vessels and or increased afferent lymph content obstructing lymphatic vessels(20). In our study, GLA induces substantial inflammation in the vaccination site and could be compromising the function of afferent lymphatics. Alternatively, it has been shown that administering DCs and inflammatory adjuvants at separate sites but within the draining area of the same DLN would result in increased accumulation of DC in DLN (21). It may be interesting to examine the effects of vaccination on tumor protection using this strategy.

The observations we made on the nature of T cell priming and expansion in the presence of GLA were also surprising. As revealed by magnetovaccination and flow cytometry data, GVAX induced strong T cell priming and expansion in the DLN. However, with the addition of GLA, significant antigen-specific T cell expansion was not seen in DLN. Instead, strong expansion of ova-specific T cells was observed systemically. Notably, vaccination formulated with GLA was associated with significant T cell accumulation in both the spleen as well as in the footpad, where the vaccine was administered. Although the antigen-specific T cell signal is reduced in the DLN, the total quantity of antigen-specific T cell expansion as measured by total body BLI signal is comparable between the two groups. Adoptive transfer of CD45.1 OT1 cells and subsequent flow cytometry analysis further

confirmed this trend. One possible scenario that could account for these findings is that GLA alters the kinetics of changes in T cell trafficking induced by vaccination such that there is decreased T cell “dwell time” in the DLN after antigen encounter, leading to rapid egress for systemic sites such as the spleen where the bulk of proliferation would occur. For vaccination in the absence of GLA, such antigen encounter would be followed by a more protracted T cell proliferative phase occurring within the DLN as revealed by the increased signals observed by BLI. However, it is important to note that the onset of priming after vaccination is not altered in the presence of GLA. Using BLI, we have confirmed that early priming on day 2-3 does not occur in any of the vaccinated groups.

Tumor growth studies showed that the augmented tumor treatment effects were observed only when GLA was administered together with GVAX. It indicates that the quality of T cell response may be different when GLA is added to the vaccine. The analysis of TILs show that more OT1 cells are homing to the tumor in mice vaccinated with GVAX+GLA (55% of the CD8 TIL) compared to GVAX (44% of CD8 TIL) or the unvaccinated mice (6% of the CD8 TIL). This show that the APC activated with GVAX+GLA although low in number are able to drive more T cells into the tumor tissues and they may have more potent anti-tumor cytotoxic effects. Previous studies have shown that TLR agonists when used as adjuvants in anti-viral vaccines are capable of driving a protective immune response by increasing the functional avidity of T cells to its antigen (22). Further, they reduce the expression of PDL-1 and regulatory T cells. Intra-tumoral administration of GLA with GVAX has shown to induce an effective tumor response by producing more potent cytotoxic T lymphocytes compared to GVAX alone (12). It is possible that the delay in tumor growth observed with GLA in the current study may be due to the combination of these effects, as well as possible systemic effects of the TLR4 agonist (although contemporaneous injection of GVAX and GLA at different anatomic sites failed to augment tumor rejection (data not shown)). Similar to our results, the requirement for GLA to be administered together with the vaccine has been previously reported for HPV vaccination in which monophosphoryl lipid A (MPL), with a related TLR4 agonist used as an adjuvant (23). The inflammation induced by MPL via the NF-κB pathway was found to be transient and not sufficient to induce activation of APCs beyond 24 hours. In our study, the timing of GLA 24 hours before and after vaccination may lead to sub-optimal activation of APC that have captured antigen.

The magnetovaccination approach of labeling APCs that have captured antigen through *in vivo* transfer mimics natural settings and enables the ability to isolate this relevant APC population. A more comprehensive analysis of the gene expression profiles of APCs that have captured antigen compared to those that have not, as well as of the impact of vaccine adjuvants on these isolated populations is ongoing. The ability to analyze these cells as a distinct population is a fundamental difference between the current study and previous studies examining adjuvant effects. The impact of the TLR4 agonist, LPS (24) and recently GLA (25) on DLN has been analyzed more globally before. For the most part, our results examining total APC populations and lymph node cellularity are in agreement with these studies, although our results are the first to have analyzed APCs that have captured antigen as a separate cell population in these studies. Lambert *et al*. showed that the administration

of GLA as a stable emulsion intramuscularly induces robust immune cell infiltration in the vaccination site (25). In addition, the number of CD11c+Gr+ cells and total number of cells in the DLN are increased with GLA treatment. We observed that the total number of CD11c + cells along with the total cellularity is increased in the DLN with GLA treatment. However, only a small proportion of these cells have captured antigens. Previously, it was shown that LPS induces increased cellularity of DLN via remodeling of high endothelial venules (HEV), which result in augmented recruitment of lymphoctyes to the DLN, where the majority of the cells are in a resting, often naivestate(24). We have verified these findings in the current model, demonstrating that DLN consists predominantly of non-proliferating cells following vaccination with both vaccines, and that the total increase in LN cellularity induced by GLA is largely attributable to an increase in non-dividing T and B cells, presumably recruited by activated endothelium (data not shown). As far as the impact of GLA on myeloid derived APC populations in the DLN, it is important to note that the absolute number of CD11c+ cells in the DLN that upregulate molecules such as MHC-II, CD40 and CD80 increases in GLA+GVAX treated mice compared to GVAX alone. However, only a small proportion of these cells have captured antigen. We cannot rule out however, that intranodal transfer of antigen to such activated cells could be undetected in our system, and potentially contribute to augmented priming(26)

Arguing against this however, is the close correlation we observed between antigen delivery to LN as measurable by MR and FACS with antigen specific T cell accumulation as measured by BLI. Finally it is most striking that APC activation as measured by increased CD40 and CD80 (and to a lesser extent, MHC II) expression was much greater in cells that have transported antigen than in their antigen negative counterparts, irrespective of the use of GLA. GVAX is known to induce APC activation markers (27) and it appears that the expression of the activation markers is already at a high level so that the addition of GLA has not further increased the level of the markers we examined. Whether other more selective measures of APC activation will differ with the use of GLA will be important to assess. Similarly, the signals responsible for APC activation associated with antigen capture remain undefined in this system. Whether similar findings are obtained with other forms of antigen (such as pure protein or peptide) will be instructive, as tumor cell-based vaccines provide a myriad of potential innate immune activators to the responding APCs.

Here magnetovaccination and MRI were used to evaluate antigen capture and APC migration to the DLN, which has potential for future clinical translation. Iron oxide nanoparticles have been used clinically to track labeled DC (15). Here, Feridex® (Endorem®)was used off-label as a superparamagnetic iron oxide (SPIO) formulation, originally approved by the FDA for human use as a liver agent. However, due to low demand and improvement of MR imaging technology to detect liver disease, it has been withdrawn from the market. In addition, studies in animal models have shown that cellular MRI can be a safe and effective tool in monitoring DC migration(28-31). Magnetovaccination has high spatial resolution, which aided in localizing the exact location of migrated APC within the DLN. APC migrated to the central medullary region of the DLN, where they meet their cognate T cells. In our previous study, we have addressed the differences between free SPIO versus APC-mediated SPIO accumulation within the DLN(14). Free SPIO particles are observed in the DLN immediately after injection resulting

in a total blackout of the DLN, while APC-internalized SPIO particles appear in the DLN within 3 days followed by a progressive increase. As we previously reported in the mouse(14), the ability to use magnetic selection of APCs that have captured antigen also provides an unprecedented opportunity to probe the relevant APC populations in clinical therapeutic cancer vaccine trials where DLN sampling is part of the biomarker assessment strategy (32)

Acknowledgments

This work was supported by NIH U54 CA151838. We thank Matthew Moake, Jie Fu and Dr. Jiadi Xu for technical inputs.

Financial support: Supported by NIH U54 CA151838 (H.I.L and J.W.M.B)

References

1. Ahrens ET, Bulte JW. Tracking immune cells in vivo using magnetic resonance imaging. Nature reviews Immunology. 2013; 13:755–63.
2. Dranoff G, Jaffee E, Lazenby A, Golumbek P, Levitsky H, Brose K, et al. Vaccination with Irradiated Tumor-Cells Engineered to Secrete Murine Granulocyte-Macrophage Colony-Stimulating Factor Stimulates Potent, Specific, and Long-Lasting Antitumor Immunity. P Natl Acad Sci USA. 1993; 90:3539–43.
3. Eager R, Nemunaitis J. GM-CSF gene-transduced tumor vaccines. Mol Ther. 2005; 12:18–27. [PubMed: 15963916]
4. Le DT, Pardoll DM, Jaffee EM. Cellular Vaccine Approaches. Cancer J. 2010; 16:304–10. [PubMed: 20693840]
5. Iwasaki A, Medzhitov R. Toll-like receptor control of the adaptive immune responses. Nat Immunol. 2004; 5:987–95. [PubMed: 15454922]
6. Schnare M, Barton GM, Holt AC, Takeda K, Akira S, Medzhitov R. Toll-like receptors control activation of adaptive immune responses. Nat Immunol. 2001; 2:947–50. [PubMed: 11547333]
7. Makkouk A, Abdelnoor AM. The potential use of toll-like receptor (TLR) agonists and antagonists as prophylactic and/or therapeutic agents. Immunopharm Immunot. 2009; 31:331–8.
8. Takeda K, Akira S. TLR signaling pathways. Semin Immunol. 2004; 16:3–9. [PubMed: 14751757]
9. Johnson DA. Synthetic TLR4-active glycolipids as vaccine adjuvants and stand-alone immunotherapeutics. Curr Top Med Chem. 2008; 8:64–79. [PubMed: 18289078]
10. Coler RN, Bertholet S, Moutaftsi M, Guderian JA, Windish HP, Baldwin SL, et al. Development and Characterization of Synthetic Glucopyranosyl Lipid Adjuvant System as a Vaccine Adjuvant. Plos One. 2011; 6
11. Baldwin SL, Shaverdian N, Goto Y, Duthie MS, Raman VS, Evers T, et al. Enhanced humoral and Type 1 cellular immune responses with Fluzone (R) adjuvanted with a synthetic TLR4 agonist formulated in an emulsion. Vaccine. 2009; 27:5956–63. [PubMed: 19679214]
12. Davis MB, Vasquez-Dunddel D, Fu J, Albesiano E, Pardoll D, Kim YJ. Intratumoral Administration of TLR4 Agonist Absorbed into a Cellular Vector Improves Antitumor Responses. Clin Cancer Res. 2011; 17:3984–92. [PubMed: 21543518]
13. Martin-Fontecha A, Sebastiani S, Hopken UE, Uguccioni M, Lipp M, Lanzavecchia A, et al. Regulation of dendritic cell migration to the draining lymph node: Impact on T lymphocyte traffic and priming. J Exp Med. 2003; 198:615–21. [PubMed: 12925677]
14. Long CM, van Laarhoven HWM, Bulte JWM, Levitsky HI. Magnetovaccination as a Novel Method to Assess and Quantify Dendritic Cell Tumor Antigen Capture and Delivery to Lymph Nodes. Cancer Res. 2009; 69:3180–7. [PubMed: 19276358]
15. de Vries IJM, Lesterhuis WJ, Barentsz JO, Verdijk P, van Krieken JH, Boerman OC, et al. Magnetic resonance tracking of dendritic cells in melanoma patients for monitoring of cellular therapy. Nat Biotechnol. 2005; 23:1407–13. [PubMed: 16258544]

16. Badr CE, Tannous BA. Bioluminescence imaging: progress and applications. Trends Biotechnol. 2011; 29:624–33. [PubMed: 21788092]
17. Lee N, Kim H, Choi SH, Park M, Kim D, Kim HC, et al. Magnetosome-like ferrimagnetic iron oxide nanocubes for highly sensitive MRI of single cells and transplanted pancreatic islets. Proc Natl Acad Sci U S A. 2011; 108:2662–7. [PubMed: 21282616]
18. Borrello I, Sotomayor EM, Cooke S, Levitsky HI. A universal granulocyte-macrophage colony-stimulating factor-producing bystander cell line for use in the formulation of autologous tumor cell-based vaccines. Human gene therapy. 1999; 10:1983–91. [PubMed: 10466632]
19. Sen D, Deerinck TJ, Ellisman MH, Parker I, Cahalan MD. Quantum dots for tracking dendritic cells and priming an immune response in vitro and in vivo. Plos One. 2008; 3:e3290. [PubMed: 18820727]
20. Liao S, Ruddle NH. Synchrony of high endothelial venules and lymphatic vessels revealed by immunization. Journal of immunology. 2006; 177:3369–79.
21. Angeli V, Ginhoux F, Llodra J, Quemeneur L, Frenette PS, Skobe M, et al. B cell-driven lymphangiogenesis in inflamed lymph nodes enhances dendritic cell mobilization. Immunity. 2006; 24:203–15. [PubMed: 16473832]
22. Zhu Q, Egelston C, Gagnon S, Sui Y, Belyakov IM, Klinman DM, et al. Using 3 TLR ligands as a combination adjuvant induces qualitative changes in T cell responses needed for antiviral protection in mice. The Journal of clinical investigation. 2010; 120:607–16. [PubMed: 20101095]
23. Didierlaurent AM, Morel S, Lockman L, Giannini SL, Bisteau M, Carlsen H, et al. AS04, an aluminum salt- and TLR4 agonist-based adjuvant system, induces a transient localized innate immune response leading to enhanced adaptive immunity. Journal of immunology. 2009; 183:6186–97.
24. Soderberg KA, Payne GW, Sato A, Medzhitov R, Segal SS, Iwasaki A. Innate control of adaptive immunity via remodeling of lymph node feed arteriole. P Natl Acad Sci USA. 2005; 102:16315–20.
25. Lambert SL, Yang CF, Liu Z, Sweetwood R, Zhao J, Cheng LL, et al. Molecular and Cellular Response Profiles Induced by the TLR4 Agonist-Based Adjuvant Glucopyranosyl Lipid A. Plos One. 2012; 7
26. Allan RS, Waithman J, Bedoui S, Jones CM, Villadangos JA, Zhan Y, et al. Migratory dendritic cells transfer antigen to a lymph node-resident dendritic cell population for efficient CTL priming. Immunity. 2006; 25:153–62. [PubMed: 16860764]
27. Kaufman HL, Ruby CE, Hughes T, Slingluff CL Jr. Current status of granulocyte-macrophage colony-stimulating factor in the immunotherapy of melanoma. Journal for immunotherapy of cancer. 2014; 2:11. [PubMed: 24971166]
28. Dekaban GA, Hamilton AM, Fink CA, Au B, de Chickera SN, Ribot EJ, et al. Tracking and evaluation of dendritic cell migration by cellular magnetic resonance imaging. Wiley interdisciplinary reviews Nanomedicine and nanobiotechnology. 2013; 5:469–83. [PubMed: 23633389]
29. de Chickera S, Willert C, Mallet C, Foley R, Foster P, Dekaban GA. Cellular MRI as a suitable, sensitive non-invasive modality for correlating in vivo migratory efficiencies of different dendritic cell populations with subsequent immunological outcomes. International immunology. 2012; 24:29–41. [PubMed: 22190576]
30. Zhang X, de Chickera SN, Willert C, Economopoulos V, Noad J, Rohani R, et al. Cellular magnetic resonance imaging of monocyte-derived dendritic cell migration from healthy donors and cancer patients as assessed in a scid mouse model. Cytotherapy. 2011; 13:1234–48. [PubMed: 21923625]
31. Dekaban GA, Snir J, Shrum B, de Chickera S, Willert C, Merrill M, et al. Semiquantitation of mouse dendritic cell migration in vivo using cellular MRI. Journal of immunotherapy. 2009; 32:240–51. [PubMed: 19242376]
32. Slingluff CL Jr, Yamshchikov GV, Hogan KT, Hibbitts SC, Petroni GR, Bissonette EA, et al. Evaluation of the sentinel immunized node for immune monitoring of cancer vaccines. Annals of surgical oncology. 2008; 15:3538–49. [PubMed: 18923873]

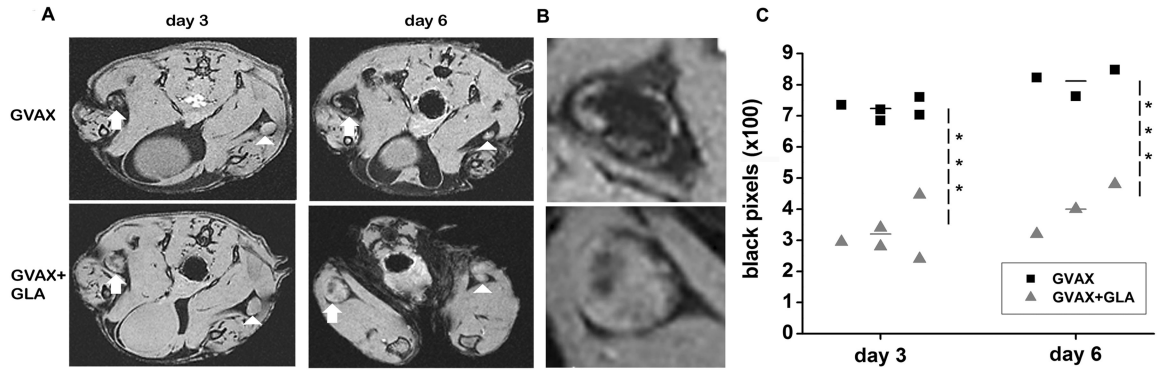

Figure 1.

GLA reduced APC mediated antigen capture and delivery to DLN. A) Axial sections through the popliteal DLN (arrow) on days 3 and 6 after vaccination show significantly less hypointensities (black pixels) in the DLN of mice vaccinated with GVAX+GLA compared to mice vaccinated with GVAX alone. Note the much smaller DLNs on the contralateral unvaccinated site (arrowhead). B) Enlarged view of the vaccinated DLNs at day 6 from panel A. C) Quantitative analysis of MRI data shows a significant reduction in black pixel count (***$p<0.001$, T-test) when GLA was added to GVAX.

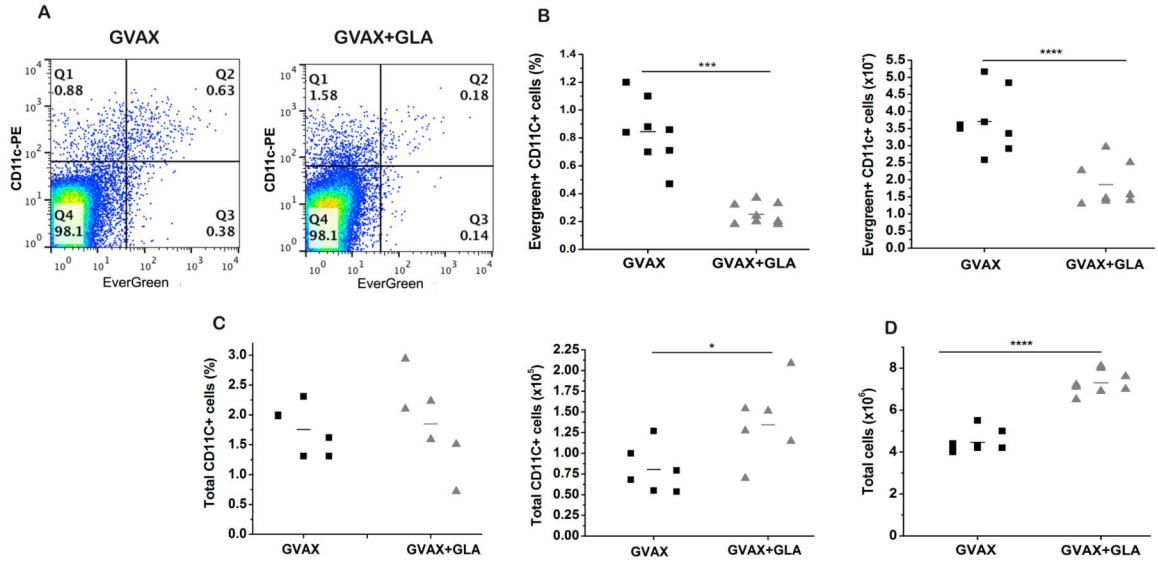

Figure 2.

Flow cytometry validates magnetovaccination. A) Flow cytometry shows reduced EverGreen+ CD11c+ cells in mice vaccinated with GVAX+GLA. B) Quantitative analysis shows a significant reduction (***p<0.001, T-test) of EverGreen+ CD11c+ cells in mice vaccinated with GLA + GVAX. C) The total number of CD11c+ cells is higher when GLA is present (*p<0.05, T-test). The total number of cells (D) was also significantly increased for GVAX + GLA (****p<0.0001, T test).

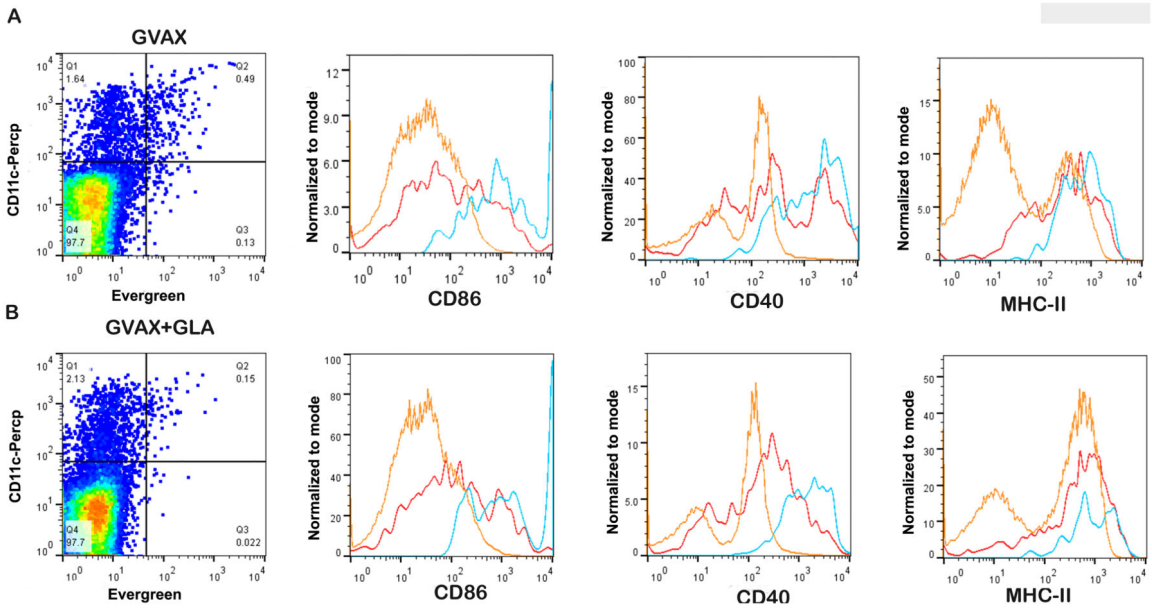

Figure 3.

Phenotypic analysis of APC activation markers in DLN on day 6. A) Representative analysis of mice vaccinated with GVAX alone (A) and GVAX+GLA (B). EverGreen+ CD11c+ cells (blue) show increased expression of activation markers CD86 and CD40 in mice vaccinated with both GVAX and GVAX+GLA compared to EverGreen-CD11c+ cells (red) and EverGreen^{-}CD11c^{-} cells (orange) in both groups. A population of EverGreen-CD11c+ cells also exhibit upregulated activation markers but not to the extent seen for EverGreen+CD11c + cells. The expression level of MHC-II in EverGreen+CD11c+ cells (blue) in both groups was comparable to EverGreen^{-} CD11c+ cells (red). The expression levels of these markers were not significantly different between the two vaccinated groups.

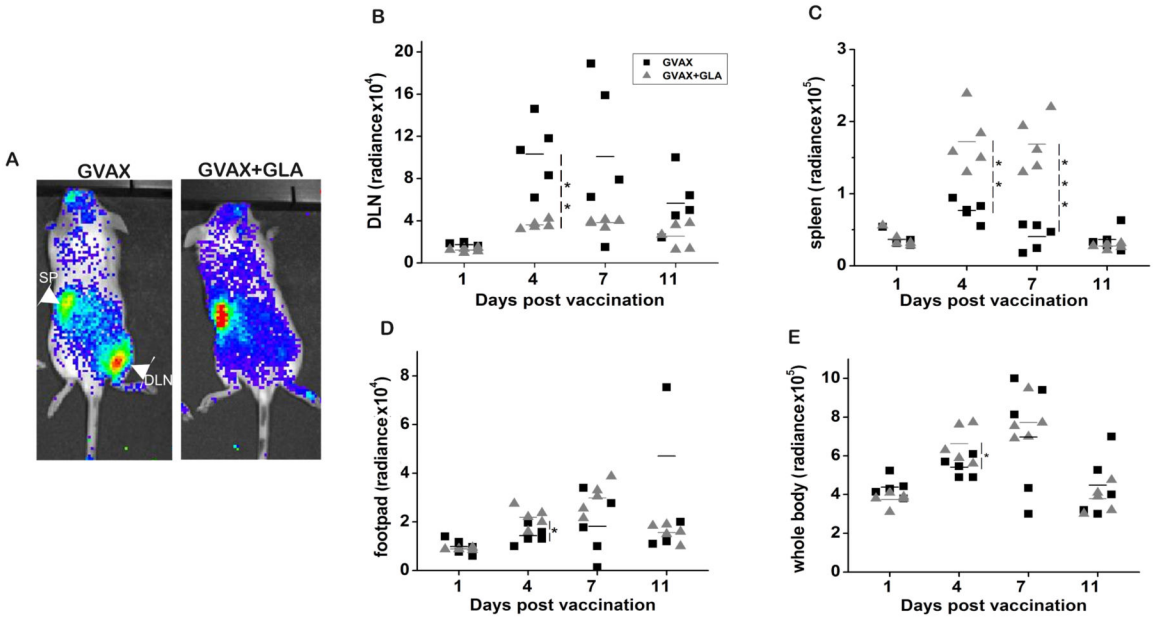

Figure 4.

Ova-specific CD8+ T cell tracking shows different patterns of T cell proliferation. A) Representative BLI at day 4 shows decreased accumulation of CD8+ T cells in the DLN of mice vaccinated with GVAX+GLA, and a strong accumulation of CD8+ T cells in the DLN of mice vaccinated with GVAX alone. A systemic pattern of expansion is observed when GLA was added to the vaccine. B) Longitudinal quantification of BLI images calculated from a ROI around the DLN shows significant accumulation of ova-specific CD8+ T cells in mice vaccinated with GVAX alone. C) Quantification of BLI signal in the spleen shows significant accumulation of transferred CD8+ T cells in the spleen of mice vaccinated with GVAX+GLA compared to GVAX alone. D) A significantly higher accumulation of CD8+ T cells was observed on day 4 in the vaccine site footpad of mice vaccinated with GVAX +GLA. E) BLI whole body signal shows an overall T cell activation and amount of proliferation that is comparable between both vaccinated groups by day 7 of vaccination. A two-tailed T test was used for statistical analysis (* $p<0.05$, ** $p<0.01$, *** $p<0.001$)

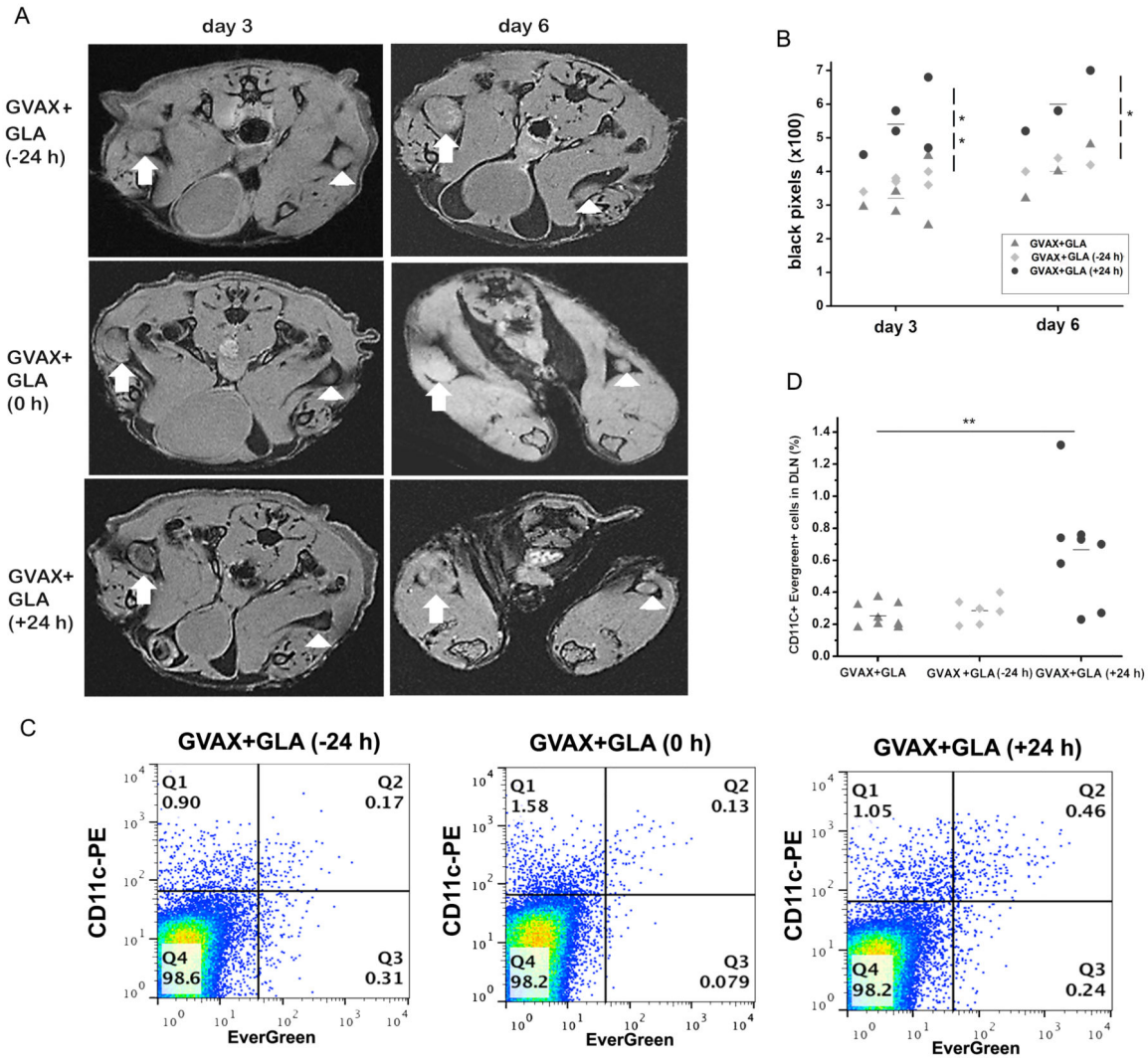

Figure 5.

Relationship between GLA timing (24 hours before, with, or 24 hours after vaccination) and antigen delivery to the DLN. A) Serial MRI sections through the popliteal nodes show an increase in black pixels in the DLN when GLA was delivered 24 hours post vaccination compared to GLA delivered together or 24 hours prior. B) MRI quantification shows a significant increase in the number of black pixels in mice treated with GLA 24 hours following vaccination on day 3 (**$p<0.01$) and on day 6 (*$p<0.05$). C) Flow cytometry analysis confirms that GLA delivered 24 hours following vaccination increase the DLN migration of DCs that have captured antigen. D) Flow cytometry data shows a significant (**$p<0.01$) increase in EverGreen+ CD11c+ cells in mice that received GLA 24 hours post vaccination.

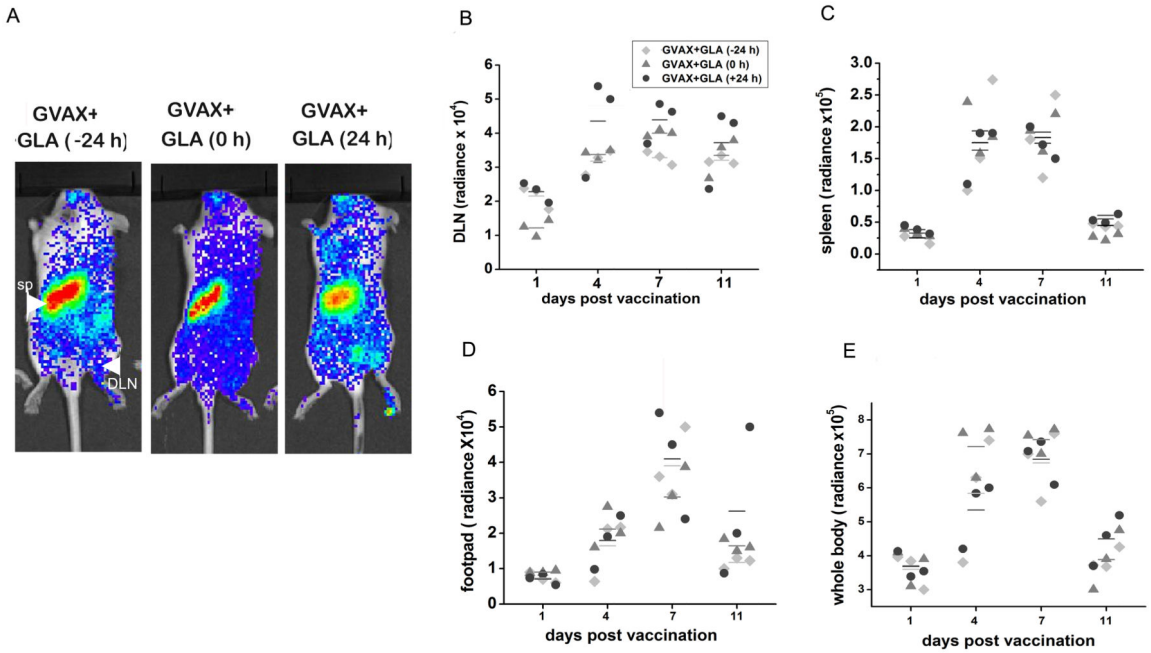

Figure 6.

Timing of GLA and dynamics of T cell proliferation. A) Representative BL images shows (site-specific) proliferation of ova- specific CD8+ T cells in vaccinated mice at day 4 after vaccination. Proliferation of T cells in the DLN is increased in mice that received GLA 24 hrs post vaccination. Unlike in mice vaccinated with GVAX alone, in GLA- treated mice, regardless of the timing, a systemic pattern of T cell proliferation is observed. B) Longitudinal quantitative analysis of BLI signals in B) DLN, C) spleen, D) footpad, and E) whole body. T cell accumulation in the spleen, footpad and whole mice were comparable between the groups.

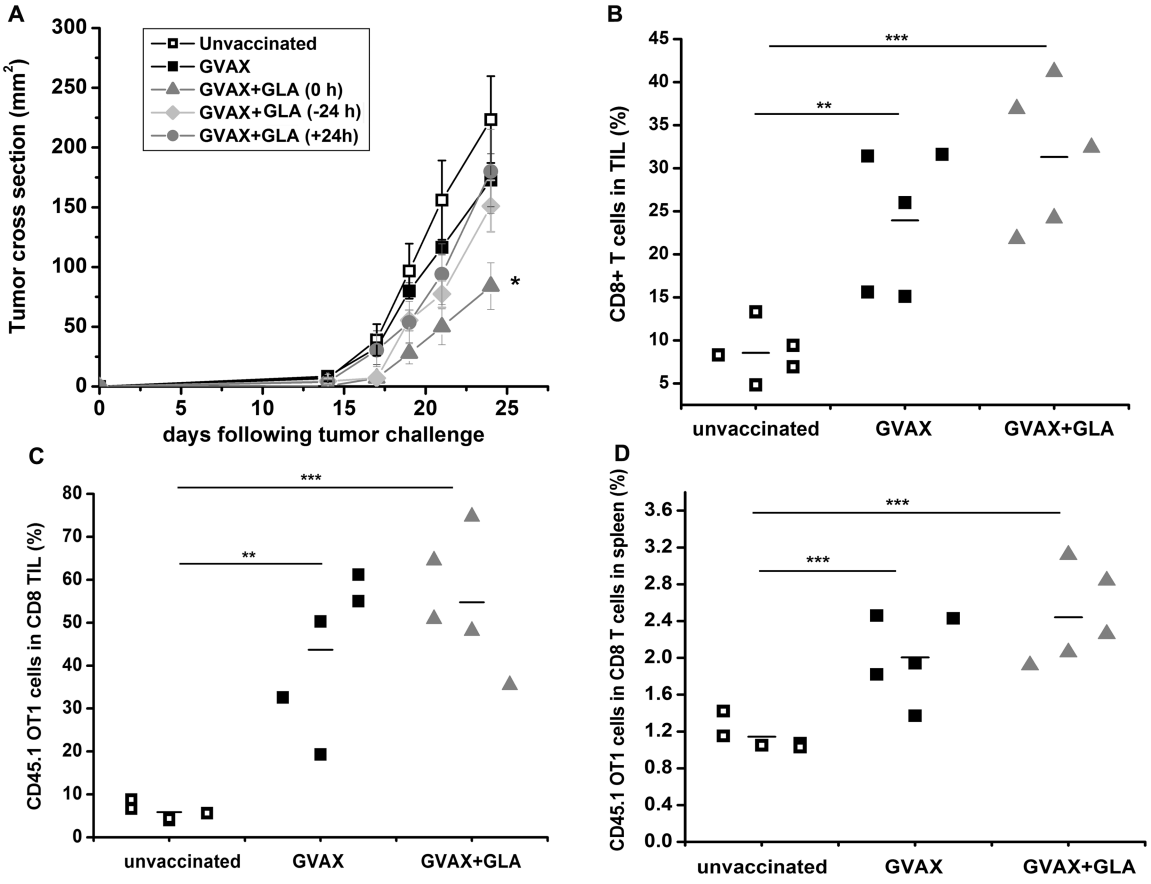

Figure 7.

Effects of vaccination on tumor growth and analysis of TILs. A) A significant delay in tumor growth was observed when GLA was administered together with GVAX (*$p<0.05$, Two-tailed T test) compared to GVAX alone or GLA administered before or after GVAX. Shown are representative data from two separate experiments (n=5 per group). B) A significant increase in vaccine-mediated T cell infiltration was observed in the GVAX+GLA group (***$p<0.001$) or the GVAX group (**$p<0.01$) compared to unvaccinated group. The increase was observed for both endogenous infiltrating $CD8^+$ T cells (B) and adoptively transferred $CD45.1^+$ OT1 T cells (C). Among the vaccinated groups, on an average GVAX +GLA induced more T cell infiltration compared to GVAX although they were not statistically significant. However, it was sufficient to induce tumor therapeutic effects (A). A similar trend was observed in the spleen (D) suggesting a strong vaccine-mediated T cell expansion in response to vaccination.